Multipole Accelerated 3-D Interconnect Analysis

K. Nabors, M. Kamon and J. White
Massachusetts Institute of Technology
Cambridge, MA 02139

1 Introduction

A wide range of integrated circuit and packaging design problems require accurate estimates of the coupling capacitances and inductances of complicated three-dimensional structures. To perform the required electrostatic or magnetoquasistatic analyses, the most commonly used approach is to apply finite-difference or finite-element techniques to a differential problem formulation. However, finite-element techniques require that the entire 3-D volume be discretized, and generating such a volume discretization for complex structures can become cumbersome. Instead, boundary or volume-element methods can be applied to solving integral formulations of the problem, in which case only boundary surfaces or conductor volumes need be discretized. Unfortunately, boundary and volume-element methods generate dense matrix problems which, if solved directly, grow in computational cost like n^3, where n is the number of elements into which the problem is discretized.

Recently, solving the dense matrices associated with boundary or volume-element methods has been made substantially more efficient through the use of iterative solution techniques accelerated by "fast-multipole" algorithms. This combined approach reduces the computational cost (and storage) of using boundary and volume-element methods to nearly $O(n)$. Below, we give a brief description of the multipole accelerated approach applied to electrostatic and magnetoquasistatic analysis. We then present results to demonstrate that the method has nearly linear computational growth, and that on realistic problems the method can be more than two orders of magnitude faster than the standard direct factorization approach.

2 Electrostatic and Magnetoquasistatic Formulation

One formulation of the electrostatic problem is to solve for conductor-dielectric and dielectric-dielectric interface charge densities, denoted $\sigma_c(x)$ and $\sigma_d(x)$ respectively, given the conductor potentials. Then for any point x on a conductor surface,

$$\psi(x) = \int_{S_c} \sigma_c(x') \frac{1}{4\pi\epsilon_0 \|x - x'\|} dS', + \int_{S_d} \sigma_d(x') \frac{1}{4\pi\epsilon_0 \|x - x'\|} dS' \tag{1}$$

where S_c and S_d are the conductor-dielectric and dielectric-dielectric interface surfaces and $\psi(x)$ is the given conductor potential. Also, for any point x on a dielectric-dielectric interface,

$$\epsilon_a \frac{\partial \psi_+(x)}{\partial n_a} - \epsilon_b \frac{\partial \psi_-(x)}{\partial n_a} = 0, \quad x \in \epsilon_a, \, \epsilon_b \text{ interface.} \tag{2}$$

where n_a is the normal to the dielectric interface, ϵ_a and ϵ_b are the permittivities of the corresponding dielectric regions, $\psi_+(x)$ is the potential at x approached from the ϵ_a side of the interface, and $\psi_-(x)$ is the analogous potential for the b side [1].

To numerically compute σ_c and σ_d, the conductor surfaces and dielectric interfaces are discretized into $n = n_c + n_d$ small panels or tiles, with n_c panels on conductor surfaces and n_d panels on dielectric interfaces. It is then assumed that on each panel i, a charge, q_i, is uniformly distributed. Finally, a system of equations is generated by insisting that (1) be satisfied at the center of each conductor panel, and that (2) be satified at the center of each dielectric panel. This leads to a system of equations of the form,

$$\begin{bmatrix} P_{11} & \cdots & P_{1n} \\ \vdots & & \vdots \\ P_{n_c 1} & \cdots & P_{n_c n} \\ E_{n_c+1, \, 1} & \cdots & E_{n_c+1, \, n} \\ \vdots & & \vdots \\ E_{n1} & \cdots & E_{nn} \end{bmatrix} \begin{bmatrix} q_1 \\ \vdots \\ q_{n_c} \\ q_{n_c+1} \\ \vdots \\ q_n \end{bmatrix} = \begin{bmatrix} \psi(x_i) \\ \vdots \\ \psi(x_{n_c}) \\ 0 \\ \vdots \\ 0 \end{bmatrix}, \tag{3}$$

where P_{ij} and E_{ij} are the potential and normal electric fields at the center of panel i due to a unit charge on panel j.

In the case of magnetoquasistatic analysis, used for extracting inductances, the conductor current density, J, satisfies $\nabla \cdot J = 0$ and for any point x in the conductor,

$$\frac{1}{\sigma}J(x) + \frac{j\omega\mu}{4\pi}\int_{V'}\frac{J(x')}{||x - x'||}dV' = -\nabla\psi(x), \tag{4}$$

where here ψ is a scalar potential, σ is the conductivity, μ is the magnetic permeability, ω is the frequency of interest, and V' is the conductor volume.

To numerically compute J, the conductor volume is discretized into b filaments, and in each filament the conductor current is assumed constant. A system of equations for the filament currents, which are denoted by the vector I_b, is then generated by insisting that at filament intersection points, the directed sum of currents associated with the intersecting filaments is zero. In addition, the filament currents must satisfy

$$ZI_b = (R + j\omega L)I_b = V_b, \tag{5}$$

where V_b, $I_b \in C^b$, b is the number of branches (number of current filaments), $Z \in C^{b \times b}$ is the complex impedance matrix, $R \in \Re^{b \times b}$ is the diagonal matrix whose elements are associated with the dc resistance of each current filament, and $L \in \Re^{b \times b}$ is the dense matrix of partial inductances [2]. Specifically,

$$L_{i,j} = \frac{\mu_0}{4\pi}\int_{filament_i}\int_{filament_j}\frac{l_i(X_i) \cdot l_j(X_j)}{|X_i - X_j|}d^3x_id^3x_j, \tag{6}$$

where $X_i, X_j \in \Re^3$ are the positions in filament i and j respectively, and $l_i, l_j \in \Re^3$ are the unit vectors in the direction of current flow in filaments i and j.

Using mesh analysis, it is possible to combine the current conservation constraint with (5) to yield

$$MZM^tI_m = V_s \tag{7}$$

where $I_m \in \Re^n$ is a vector of mesh currents, $M \in \Re^{n \times b}$ is the mesh matrix, V_s is the mostly zero vector of source voltages, and n is the number of meshes.

3 The Multipole-Accelerated Approach

If an iterative algorithm, typically GMRES [3], is used to solve either (3) or (7), then each iteration of the algorithm will cost n^2 operations. This is because the matrices in (3) and (7) are dense, and therefore evaluating candidate solution vectors involves a dense matrix-vector multiply. However, in both (3) and (7), multiplying by the associated matrix is equivalent to evaluting a potential at n points due to n sources. This computation can be performed in order n operations using the fast multipole algorithm [4].

As a brief explanation of how the fast multipole achieves such efficiency, consider two configurations, depicted in 2-D for simplicity, given in Figs. 1 and 2. In either figure, the obvious approach to determining the electrostatic potential at the n_1 evaluation points from the n_2 point-charges involves $n_1 * n_2$ operations; at each of the n_1 evaluation points one simply sums the contribution to the potential from n_2 charges. An accurate approximation for the potentials for the case of Fig. 1 can be computed in many fewer operations using *multipole expansions*, which exploit the fact that $r >> R$ (defined in Fig. 1). That is, the details of the distribution of the charges in the inner circle of radius R in Fig. 1 do not strongly effect the potentials at the evaluation points outside the outer circle of radius r. It is also possible to compute an accurate approximation for the potentials at the evaluation points in the inner circle of Fig. 2 in many fewer than $n_1 * n_2$ operations using *local expansions*, which again exploit the fact that $r >> R$ (as in Fig. 2). In this second case, what can be ignored is the details of the evaluation point distribution.
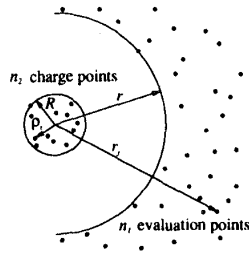
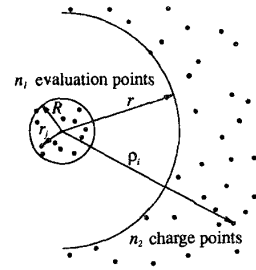Figure 1: Exploiting charge clusters using multipole expansions.

Figure 2: Exploiting evaluation point clusters using local expansions.
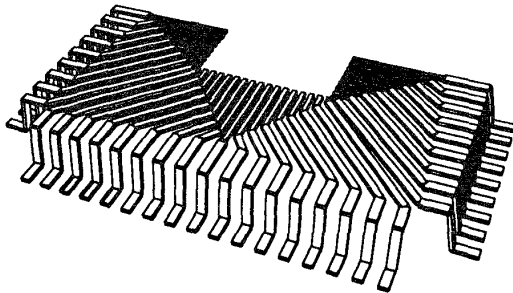

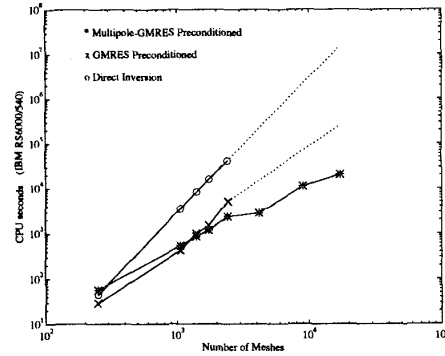Figure 3: Half of a pin-connect structure. Thirty-five pins shown.

Figure 4: CPU times (IBM RS6000/540).

4   Results

In this section, we present results from the multipole-accelerated electrostatic and magnetoquasistatic analysis programs FASTCAP2 [5] and FASTHENRY [6]. To begin, consider a typical industrial example, a 35-pin package shown in Figure 3. The cost of computing the associated inductance matrix using direct factorization, GMRES, and multipole-accelerated GMRES, as a function of discretization refinement is show in Figure 4. Note the for a $10,000$ filament discretization, which is barely sufficient to properly model finite penetration depth and proximity effects, the multipole accelerated algorithm is two orders of magnitude faster than direct factorization, and an order of magnitude faster than explicit GMRES.

For the example package, the mutual inductance between pins 1 and 2 (labeled clockwise from the right) is much larger than the mutual inductance between pins 1 and 35. To show that the approximations used by the fast multipole algorithm are sufficiently well-controlled to make it possible to accurately compute the small coupling inductances, consider the results in Table 5. The mutual inductance between pins 1 and 35 is more than two orders of magnitude smaller than the mutual inductance between pins 1 and 2, yet the solution computed using the multipole-accelerated algorithm is still within one percent of the solution computed using direct factorization.

The connector problem in Figure 7 and the DRAM cells in Figure 8 are examples of structures that can be analyzed with FASTCAP2, which uses a multipole-accelerated boundary-element method. For the connector, the U-shaped polyester body has a relative permittivity of 3.5. Note that for the DRAM cells, the dimples in the ground plane below the bit line vias model the drain to substrate capacitors. Also, the upper aluminum word lines are covered with a silicon nitride passivation layer with relative permittivity 7.0. Below the passivation layer is silicon dioxide, with relative permittivity of 3.9.

74

pin pair	direct	gmres	multipole
1 to 2	3.0107e-02	3.0106e-02	3.0082e-02
1 to 35	2.0847e-04	2.0838e-04	2.0678e-04

Figure 5: Inductance accuracy comparison.

	DRAM	Connector
cond. panels	4881	6464
dielec. panels	1248	3060
total panels	6129	9524
FASTCAP2 CPU minutes	17	30
Direct CPU minutes	(1300)	(4900)

Figure 6: CPU times (IBM RS6000/540). Times in parentheses are extrapolated.
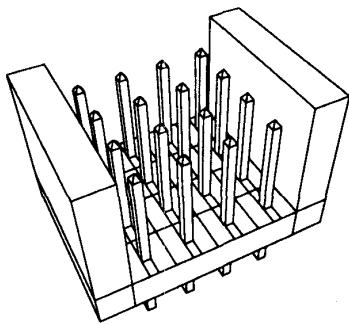
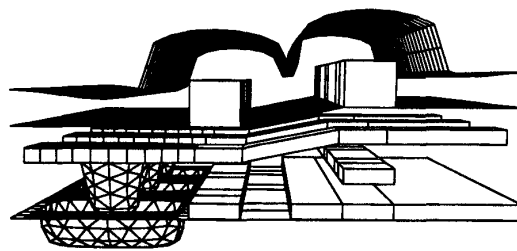Figure 7: A backplane connector example.

Figure 8: Neighboring DRAM cells.

5 Conclusions and Acknowledgements

Combining boundary and volume-element methods with multipole-accelerated iterative methods leads to very efficient programs for extracting capactances and inductances of complex 3-D structures. The authors would like to thank Songmin Kim, Dr. Sami Ali, and Joel Phillips for their help in understanding inductance. This work was supported by the Defense Advanced Research Projects Agency contract N00014-91-J-1698, the National Science Foundation contract (MIP-8858764 A02), and grants from I.B.M. and Digital Equipment Corporation.

References

[1] S. M. Rao, T. K. Sarkar, and R. F. Harrington, "The electrostatic field of conducting bodies in multiple dielectric media," *IEEE Transactions on Microwave Theory and Techniques*, vol. MTT-32, pp. 1441–1448, November 1984.

[2] P. A. Brennan, N. Raver, and A. Ruehli, "Three dimensional inductance computations with partial element equivalent circuits," *IBM Journal of Res. and Develop.*, vol. 23, pp. 661–668, November 1979.

[3] Y. Saad and M. H. Schultz, "GMRES: A generalized minimal residual algorithm for solving nonsymmetric linear systems," *SIAM Journal on Scientific and Statistical Computing*, vol. 7, pp. 856–869, July 1986.

[4] L. Greengard, *The Rapid Evaluation of Potential Fields in Particle Systems*. Cambridge, Massachusetts: M.I.T. Press, 1988.

[5] K. Nabors and J. White, "Multipole-accelerated capacitance extraction algorithms for 3-d structures with multiple dielectrics." To appear in *IEEE Transactions on Circuits and Systems—I: Fundamental Theory and Applications*.

[6] M. Kamon, M. Tsuk, C. Smithhisler, and J. White, "Efficient techniques for inductance extraction of complex 3-d geometries," in *Proceedings of Int. Conf. on Comp. Aided Design*, November 1992.